Fermi National Accelerator Laboratory

FERMILAB-TM-2089

Production and Release of Airborne Radionuclides Due to the Operation of NuMI

Nancy L. Grossman, David J. Boehnlein and J. Donald Cossairt

Fermi National Accelerator Laboratory
P.O. Box 500, Batavia, Illinois 60510

August 1999

Operated by Universities Research Association Inc. under Contract No. DE-AC02-76CH03000 with the United States Department of Energy

Production and Release of Airborne Radionuclides Due to the Operation of NuMI

Nancy L. Grossman, David J. Boehnlein, and J. Donald Cossairt

August 1999

A. Introduction

The operation of the NuMI beamline will result in the production of significant quantities of airborne radionuclides due to the large proton beam intensities to be delivered to this facility. In this report we predict the production of airborne radionuclides and their release to the environment during NuMI operations[1]. An estimate is provided of the maximum dose equivalent that might be delivered by this pathway to a hypothetical individual continuously present at the Fermilab site boundary. Likewise, the dose equivalent rate due to exposure to activated air within the NuMI target station enclosure is estimated. It is concluded that the airborne radioactivity produced in the course of NuMI operations will be in compliance with applicable Federal and State regulations.

B. Summary of Regulatory Requirements

Federal regulations, which are further implemented by the State of Illinois, govern the releases of airborne radionuclides, excluding radon and radon progeny, by U. S. Department of Energy Facilities (CFR89)[2]. These regulations place an annual limit of 10 mrem/year on the dose equivalent that can be delivered to a member of the public due to the release of airborne radionuclides from DOE facilities. The methodology for determining the dose equivalent is also specified. The regulations further require the application of continuous monitoring in accordance with U. S. Environmental Protection Agency specifications if the dose equivalent should exceed 0.1 mrem/year. Requirements for monitoring systems that meet these specifications are quite stringent and could tightly constrain Fermilab operations. For example, a failure of the monitoring system might well require suspension of operations pending its repair. Maintaining the total site boundary dose equivalent to be less than 0.1 mrem/year permits the Laboratory to measure these releases as a part of a confirmatory monitoring program. This program is generally, but not necessarily, operated continuously. It does not require the suspension of facility operations during short periods when the monitoring system may be unavailable. It has been standard practice for the Fermi National Accelerator Laboratory to be considered as a single facility under this regulation. Thus, these limits apply to the total release from the Laboratory. This choice has been made to permit Fermilab to comply with the regulation while maintaining the flexibility to alter the locations of operations throughout the facility in order to meet the needs of the physics research program.

---

[1] Air releases due to beam loss in the Main Injector extraction region are not within the scope of this paper.

[2] Dagenais (Da84) has provided estimates of the buildup of radon in tunnels made of the rock found at the level of the NuMI facilities on the Fermilab site. These results, including worst case estimates, indicate occupational exposure to radon and radon progeny under the ventilation conditions present in the NuMI facility to be unimportant compared to the applicable regulatory limits of (CFR93).

A dose equivalent rate of 0.1 mrem/year or less, approximately distributed uniformly throughout several months, cannot feasibly be measured directly. The alternative indirect method used to estimate such a dose equivalent consists of measurements of the activity released from the various sources using stack monitors at the release points. The activity released, expressed in terms of the individual radionuclides found at the stacks, is then used as input in the computer code CAP88-PC along with specified meteorological data for the calendar year during which the releases occurred. This computer code, required by the applicable regulations (CFR89), calculates the dose equivalent delivered at the Fermilab site boundary. It employs a Gaussian plume model to determine the effects of diffusion and radioactive decay upon average concentrations of radionuclides, and hence the dose equivalent, at offsite locations. The results fluctuate from year-to-year due to details of the Fermilab operational schedule and variations in meteorological parameters used as input data. During CY 1996, 21 Ci were released from the Laboratory and a dose equivalent at the site boundary of 0.013 mrem was calculated. During this period, the Fermilab Fixed Target program was operating with 800 GeV protons along with simultaneous operations of the Antiproton source that used 120 GeV protons. Similar operations during CY 1997 resulted in 0.015 mrem dose equivalent due to the release of 29.5 Ci. During this period, the releases of airborne radioactivity occurred in the same general portion of the Fermilab site as will those due to NuMI operations. The average of these results for the site boundary yields a dose equivalent per unit activity of 5.64×10^{-4} mrem/Ci, a scaling factor that can be used to predict conditions found during NuMI operations.

Consistent with these requirements, in March 1999, Fermilab submitted an application renewal to the Illinois Environmental Protection Agency for its lifetime air pollution operating permit[3]. This application addressed the radionuclide emissions from NuMI and other Fermilab facilities. It specified that the doses to the public will be kept well below 0.1 mrem/year for all Fermilab operations. The average annual activity release is to be kept less than 100 Ci. In consideration of the overall program of operations at Fermilab, the NuMI project management in consultation with the staff of the Environment, Safety, and Health Section established an administrative goal for the NuMI project of a maximum annual release of 45 Ci. The corresponding maximum anticipated dose equivalent due to NuMI operations that might be received by an individual hypothetically present full-time at the Fermilab site boundary is estimated to be 0.025 mrem.

C. The Physics of the Production and Release of Airborne Radionuclides at an Accelerator

The production of airborne radioactivity has been discussed elsewhere in detail (Co99). Thus, only summary results will be given here. Table 1 gives the volume percentages by atoms for the most abundant stable nuclides in the atmosphere along with the corresponding values of the atom number densities, N_j. These atoms are the principal targets for the nuclear reaction processes that produce the airborne radioactivity.

[3] In response to this application, Illinois Environmental Protection Agency permit was issued on June 16, 1999.

Table 1 Abundances of the Most Common Stable Nuclides in the Atmosphere

Isotope	Percentage by volume in the atmosphere (atoms)	N_j (atoms cm^{-3}) at room temperature
^{14}N	78.16	4.199×10^{19}
^{16}O	20.00	1.075×10^{19}
^{40}Ar	0.467	1.558×10^{17}
^{15}N	0.290	2.149×10^{16}
^{18}O	0.040	1.255×10^{17}

The result of experience at Fermilab and other high energy proton accelerators is that the high energy hadrons present in the beam and the beam spray produce the short-lived radionuclides ^{11}C, ^{13}N, and ^{15}O as well as ^{3}H. Other radionuclides are also produced by the interactions of high energy hadrons with the constituents of air. However, they generally neither represent an important consideration in occupational radiation protection nor form a major component of the eventual release of radioactivity to the environment. The production of ^{7}Be due to interactions with these most abundant target atoms is also a possibility, but this radionuclide has never been detected in the releases from target stations at Fermilab, probably due to its plating out on beamline components. It is therefore not further considered with respect to the release of airborne radioactivity to the environment. Spallation reactions on the oxygen and nitrogen atoms represent the dominant physical process.

An important secondary process is the capture of thermal neutrons in the ^{40}Ar(n_{th},γ)^{41}Ar reaction. Despite the relatively small abundance of ^{40}Ar target atoms in air, this reaction can be important due to its large cross section of 660 mb at the most probable room temperature thermal neutron energy of 0.025 eV. The production of ^{41}Ar has been seen in configurations where large iron shields are bare; that is, not covered by hydrogeneous materials like concrete. Under these conditions, the neutron energy spectrum is dominated by a high flux density near one MeV (El86). These low energy neutrons, then, readily thermalize in the open volume and thus promote the production of ^{41}Ar. Conversely, this particular radionuclide is not seen in situations in which the steel core of a particular target station is completely covered with a hydrogeneous material (typically concrete) without an intervening layer of air. In some of the same situations in which the ^{41}Ar is seen, ^{38}Cl and ^{39}Cl are also observed at lower concentrations, likely due to the ^{40}Ar(γ,pn)^{38}Cl and ^{40}Ar(γ,p)^{39}Cl reactions, respectively. The capture of thermal neutrons by various materials present in the enclosure generally provides a copious source of photons that proceed to produce the chlorine isotopes. Results of this type have been reported by Butala et al. (Bu89) and by Vaziri et al. (Va93, Va94). It appears that care taken to minimize the thermalization of neutrons minimizes the contribution of the argon and chlorine isotopes. The estimation of thermal neutron flux densities is a rather difficult calculation. In the remainder of this report, the value of the concentration of ^{41}Ar is taken to be 2.5 % of the sum of the concentrations of ^{11}C and ^{13}N calculated within a given enclosure. The production of the chlorine isotopes is likely to be insignificant. This choice is conservative in that typical values of only one per cent are commonly found in measurements conducted at Fermilab.

Patterson and Thomas (Pa73) have expanded the general activation equation to derive the total specific activity, *S* of an enclosed volume of radioactive air during an irradiation uniformly distributed in time;

$$S = C\sum_i \left[\sum_j \phi_\gamma N_j \bar{\sigma}_{ij_\gamma} + \sum_j \phi_{th} N_j \bar{\sigma}_{ij_{th}} + \sum_j \phi_{HE} N_j \bar{\sigma}_{ij_{HE}} + \right] [1 - \exp(-\lambda_i t_{irrad})] \exp(-\lambda_i t_{cool}). \qquad (1)$$

The inner summation (index *j*) is over the atom densities of the target elements, N_j (atoms cm^{-3}). The outer summation (index *i*) is over *i* radionuclides of concern, each with its decay constant, λ_i (s^{-1}). $\phi\gamma$, ϕth, and ϕ_{HE}, represent the average photon, thermal neutron and high energy hadron flux densities. These must be obtained through semi-empirical formulae or by means of a Monte Carlo calculation. When used in this equation, these are averaged over a suitable spectral region and over a corresponding volume. Averaging of fluctuations in the flux density due to variations in the beam intensity during the irradiation time is also implicit. In this equation t_{irrad} is the irradiation time while t_{cool} represents the decay time following the cessation of the irradiation. In the remainder of this paper, only the high energy summation is actually calculated. The production of ^{41}Ar due to thermal neutron capture is calculated indirectly, as discussed. The $\bar{\sigma}_{ijHE}$ values were taken from the available literature.

These cross sections, denoted simply as σ_{HE} hereafter, can be regarded to good approximation, as being independent of energy above the appropriate spallation reaction thresholds of a few tens of MeV. The constant, *C*, is the conversion to specific activity and is equal to unity for activity in Bq cm^{-3} and 2.7027 x 10^{-11} for activity in Ci cm^{-3}.

Adjustments for the presence of ventilation can conveniently be made for a given radionuclide (Co99). Temporarily dispensing with the index, *i*, one uses an effective decay constant, λ', that includes the physical decay constant, λ, in addition to a ventilation term, *r*,

$$\lambda' = \lambda + r, \qquad (2)$$

$$\text{where} \qquad r = \frac{D}{V}.$$

D is the ventilation rate in air volume per unit time and *V* is the volume in which the mixing occurs. Thus *r* is the number of air changes per unit time. With mixing, the specific activity as a function of irradiation time for a single radionuclide, $a'(t_{irrad})$, is given by,

$$a'(t_{irrad}) = \frac{\lambda N \sigma_{HE} \phi_{HE}}{\lambda + r} \{1 - \exp[-(\lambda + r) t_{irrad}]\} \qquad (3)$$

But the product $N\sigma_{HE}\phi_{HE}$ is just the saturation concentration, a_{sat}, obtained after an "infinite" irradiation period without mixing in units of Bq cm^{-3}. Hence, with mixing and an infinite irradiation time, the saturation concentration, a'_{sat} reaches:

$$a'_{sat} = \frac{\lambda\, a_{sat}}{\lambda + r}. \qquad (4)$$

As an additional ingredient, if the ventilation system is set up to provide a finite travel time, $t_{transit}$ from the production region to the release point, the concentrations released at the latter location, a_{rel}, will be given by,

$$a_{rel} = \frac{\lambda N \sigma \phi}{\lambda + r}\{1 - \exp[-(\lambda + r)\, t_{irrad}\,]\}\exp(-\lambda\, t_{transit}). \qquad (5)$$

An enclosure containing airborne radionuclides could, in principle, be kept sealed up during operations and for a time, t_{cool}, following suspension of operations to allow for decay before the initiation of rapid mixing and release. If this approach is taken, then the corresponding value of t_{cool} should be added to that of $t_{transit}$ in the argument of the last exponential function of Eq. (5). For the radionuclides considered here, the expression in the middle of the equation enclosed within the braces is significantly less than unity only for ^{3}H and ^{7}Be. For all others, saturation is readily achieved during a relatively short period of operations of only a few hours. Using the rate of air release and the other parameters described above, one can calculate the total release, in terms of activity, of each individual radionuclide over some period of time. One does this by multiplying this specific activity, a_{rel}, by the volume of air released during the same period.

Table 2 gives values of decay constants and production cross sections. The production cross sections are conservative choices taken from the references by Barbier (Ba69) and Thomas and Stevenson (Th88).

Table 2 Physical Parameters for Typical Radionuclides Produced in Air at a High Energy Proton Accelerator

	Decay Constants, λ_i, and High Energy Cross Sections, σ_{ijHE} (mb) for the Production of Various Radionuclides					
Product =>	**^{3}H**	**^{7}Be**	**^{11}C**	**^{13}N**	**^{15}O**	**^{41}Ar[4]**
λ (sec^{-1}) =>	1.79 x 10^{-9}	1.51 x 10^{-7}	5.69 x 10^{-4}	1.16 x 10^{-3}	5.67 x 10^{-3}	1.05 x 10^{-4}
Target Nuclide	**High Energy Hadron Cross Sections, σ_{HE} (mb)**					
^{14}N	30	14	20	4	0	
^{16}O	30	8	10	5	35	
^{40}Ar	1	10	1	1	1	
^{15}N	30	14	20	4	0	
^{18}O	30	8	10	5	35	

[4] The production of ^{41}Ar by means of thermal neutron capture is handled in an *ad hoc* manner. See discussion in the text.

D. General Description of the NuMI Facility Ventilation System

The planned NuMI facility has been described in detail elsewhere (NuMI98). The exact details of facility design are expected to evolve somewhat as the project develops, but the major features are well-covered by (NuMI98). The NuMI facility is largely located deep underground relative to other facilities at Fermilab. Figure 1 summarizes the configuration of the facility with respect to the ventilation system. A major portion of the facility will be located in an aquifer, with resultant levels of rather high relative humidity. With respect to the subject of this paper, the facility can be divided into four regions. These are the Pretarget Region, the Target Hall, the Decay Region, and the Hadron Absorber. For the present calculations and all others associated with NuMI radiation issues, the incident beam of 120 GeV protons is taken to be a pulse of 4×10^{13} protons every 1.9 second. The total annual delivery of 3.7×10^{20} protons will be over an "operational year" of 1.75×10^{7} seconds. For the purposes of these calculations, the average duration of an irradiation period between accelerator maintenance shutdowns was taken to be t_{irrad} = 720 hours (30 days). The cooling time, t_{cool}, unless noted otherwise, was taken to be zero. The results are not sensitive to this particular choice of the value of t_{irrad} since the dominant radionuclides produced have lifetimes small compared to all reasonable irradiation times.

Given the levels of humidity anticipated to be present in the tunnels, it is believed to be necessary to provide continuous ventilation of the facility to minimize corrosion of the highly radioactive beam transport components and their possible premature failure. Thus, the alternative of providing no significant ventilation during operations and allowing for a period of decay prior to release to the environment was rejected in order to reduce this possible cause of failure of these components. A benefit of this approach is the minimization of the occupational radiation exposures due to repair work on these components.

The ventilation system has been designed to maximize, where possible, the transit times to the ventilation stacks. For comparison with the engineering design, ventilation flow rates are given in units of $ft^3\ min^{-1}$(cfm) (1 $ft^3\ min^{-1}$ = 471.95 $cm^3 s^{-1}$). Air enters the Target Hall at the NuMI Target Service Building located above the Target Hall. The present design provides for a nominal air flow rate of 650 cfm moving upstream from the target station and released at the upstream end of the Pretarget Region. An approximate travel time of 60 minutes for the air moving through this region results from this flow rate. The air in the Carrier Pipe will not be vented. Likewise, the ventilation system provides for a nominal air flow rate of 1500 cfm past the target in the downstream direction. This air continues through the Decay Region to the ventilation stack located at about half the distance to the beam absorber where it is released to the environment after a total travel time of approximately 180 minutes (3 hours). At this halfway point, a fire wall completely separates this ventilation system from that provided for the downstream half of the Decay Region and the Hadron Absorber. At the MINOS access shaft, air is supplied at the nominal rate of 2250 cfm with a transit time of approximately 120 minutes (2 hours) from the Hadron Absorber to the ventilation stack. The air supplied to the MINOS experimental hall is kept completely separate from the air ventilating the Hadron Absorber. Beyond the Hadron Absorber, there are no radioactivation issues since, by design, there are essentially no hadrons present. This design attains the objective of keeping the air in the MINOS Experimental Hall free of radionuclides in view of its availability for continuous occupancy during operations of the facility.

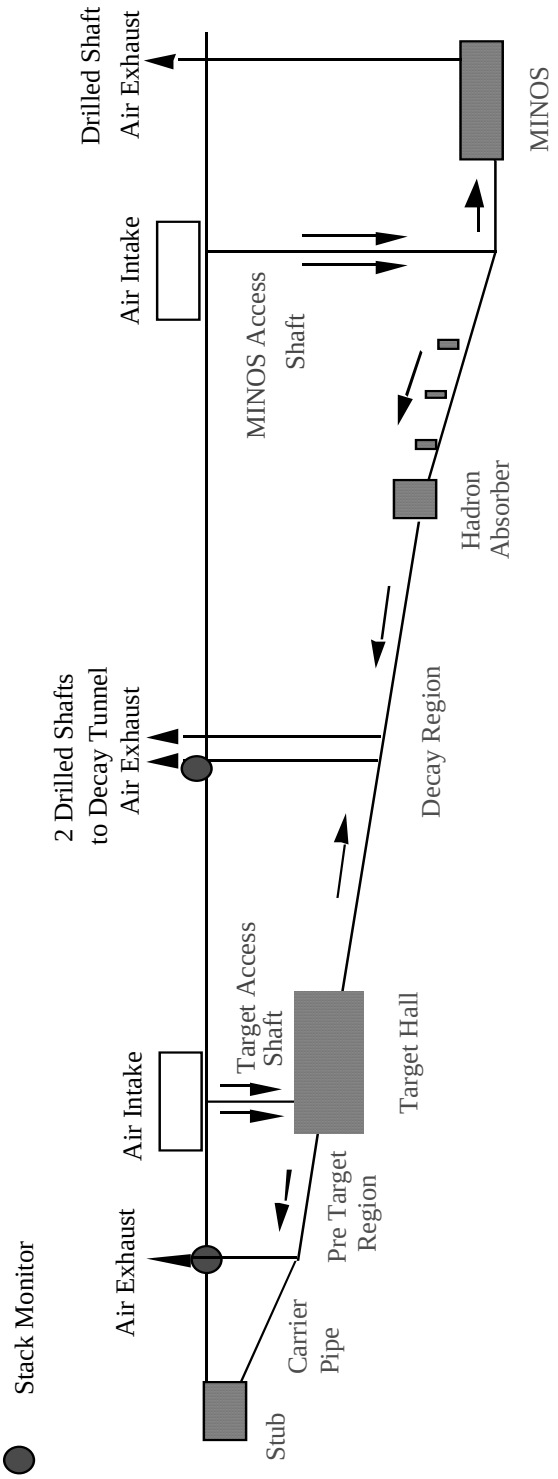

Figure 1 Longitudinal schematic elevation view of the NuMI facility on the Fermilab site showing the significant features of the ventilation and air monitoring systems. Nominal flow rates are 650 cfm in the Pretarget Region, 1500 cfm in the first half of the Decay Region, and 2250 cfm in the second half of the Decay Region. The air in the Carrier Pipe will not be regularly vented to the atmosphere. In the Decay Region, the air flow moving downward from the Target Hall is separated completely from that moving upward from the Hadron Absorber. The air moving toward the MINOS Experimental Hall is not subject to activation.

Pretarget Region

Lucas has estimated that the fraction of the proton beam that might be lost on beamline components in the Pretarget Region will be between 10^{-4} and 10^{-5} (Lu99). Further study of the beam loss profile, and its radiological consequences, is the subject of a planned future study (Mo99). For present purposes here, one needs to estimate the high energy flux density to be used in Eq. (1). The results of two different calculations are used to obtain such an estimate. Schopper et al. (Sc90) have published the results of a large number of Monte-Carlo calculations for "generic" situations using the FLUKA code (Aa86). Specifically, they have obtained results for the situation in which a copper target of 1 cm diameter, 10 cm length was bombarded by 100 GeV protons. The target was located on the axis of a cylindrical tunnel 100 meters long and 200 cm in radius [Fig. 2.41e, p. 119 of ref. (Sc90)]. In this calculation, the initial interactions were modeled to occur 10 meters deep (longitudinally) in the tunnel. The result was that the hadron star density at the inner surface of the wall ranged from peak value of approximately 1.5×10^{-7} stars $cm^{-3}proton^{-1}$ over a region about 10 meters long. For the remainder of the tunnel, a value of about 3×10^{-8} stars cm^{-3} $proton^{-1}$ resulted. The contours of equal star density for this calculation indicate essentially no further dependence on distance along the tunnel wall measured downstream of the target. Thus, the results due to this "point" interaction of the primary protons is regarded as approximating the results one might obtain if the same number of protons were to be lost uniformly over the entire length of the Pretarget Region.

An alternate estimate was obtained from another calculation reported by these same authors. The second calculation was performed for 100 GeV protons striking a 2 cm radius beryllium target, 0.1 cm long, contained within a vacuum pipe inside of a 10 meter long magnet. The beam axis coincided with that of a concrete tunnel 100 meters long and 150 cm in radius [Fig. 2.46b, p. 123 of ref. Sc90]. The initial interactions were modeled to occur 10 meters longitudinally deep in the tunnel. In this situation, the calculated star density ranged from 1.0×10^{-7} to 1.5×10^{-7} stars cm^{-3} $proton^{-1}$ over the entire length of 90 meters following the initial interactions. As before, the weak longitudinal dependence of the star density along the tunnel wall leads one to take the resulting pattern of radiation to be similar to those anticipated for a uniform loss along the entire Pretarget Region. Given the results of these "generic" calculations, it is reasonable to adopt a value of 1×10^{-7} stars $cm^{-3}proton^{-1}$ in the concrete at the inner surface of the wall.

This result will now be used to estimate the air activation due to stray beam losses in the Pretarget Region that will largely be due to the "tails" of the beam envelope striking beam transport components and diagnostic instrumentation. While some beam loss may be distributed throughout the Pretarget Region, most of the beam loss is likely to occur on beam transport elements near the upstream end (Lu99). Given the weakness of the longitudinal dependence of star density due to beam losses of this general type, the results are not strongly sensitive to the exact location of the proton interaction with beam transport components. From the results discussed above, the irradiation of air in the tunnel is approximately uniform, and independent of longitudinal position. This enclosure can be approximated as a cylinder of equivalent cross-sectional area. In the present design, the radius of such an equivalent cylinder ranges from about 160 to 190 cm at various points within the Pretarget Region. Thus, the radii of the tunnels

addressed in the calculations reported by Schopper et al. are approximately equivalent to the NuMI Pretarget Region. Since the above calculation was performed for a proton energy E, of 100 GeV protons, one should scale by the "Moyer" energy scaling of $E^{0.8}$ to get a value of star density appropriate for E = 120 GeV. The result is a value of 1.75 x 10^{-7} stars cm^{-3} $proton^{-1}$.

It is now necessary to estimate the flux density of high energy particles in the air within the enclosure. The flux density of high energy particles in the concrete wall, ϕ_{HE}, is related to the star density in the concrete wall, S_D, through the following;

$$\phi_{\mathrm{HE}} = \lambda_{\mathrm{int}}\, S_D\,, \tag{6}$$

where λ_{int} is the high energy value of the nuclear interaction length of concrete, customarily tabulated (e.g., by the Particle Data Group) and here taken to be 41.6 cm after taking into account the density of typical concrete of 2.4 g cm^{-3}. In the air in the neighborhood of the innermost layer of the concrete, this flux density will have the same value and includes all high energy hadrons. Evaluating this at the wall, one obtains from the above estimates the value ϕ_{HE} (wall) = 7.3 x 10^{-6} cm^{-2} $proton^{-1}$. The ingredient needed for the calculation of air activation in this region is the flux density averaged over the cylinder that approximates the tunnel. It is easy to show that this value is twice that found at the wall if the radial dependence is assumed to be proportional to $1/r$. Thus, we can take ϕ_{HE} = 1.5 x 10^{-5} cm^{-2} $proton^{-1}$. This flux density should be correct to within a factor of about 2 for beam losses of this type.

The air in this enclosure is to be ventilated at a constant rate, nominally 650 cfm, in a flow that can be taken to be laminar[5]. Under such non-diffusive conditions, the following continuity equation describes the concentration of a given radionuclide, C, as a function of longitudinal distance, z, and time, t,

$$\frac{\partial C(z,t)}{\partial t} + v\frac{\partial C(z,t)}{\partial z} + \lambda\, C(z,t) = P(z,t)\,, \tag{7}$$

where v is the velocity of the air movement and $P(z,t)$ is the rate of production of the given radionuclide as a function of position, z, and time, t. On the left hand side, the last term represents the decay while the middle term describes transport from one location to another. Since, as discussed above, $P(z,t)$ has essentially no dependence on z, then $C(z,t)$ likewise has no significant z-dependence so that the solution reduces to that of Eq. (1) and the concentration throughout the volume of the Pretarget Region is approximately constant. Thus, the concentrations of the radionuclides can be calculated using Eq. (1). The annual release can, then, simply be determined by multiplying these concentrations by the ventilation rate, converted to appropriate units, and multiplied by the duration of the operational year defined previously. The results are plotted in Figure 2 as a function of air release rate for the beam loss fraction of 10^{-4}, the upper limit of the range estimated by Lucas. No decay in transit up the ventilation stack is included in the results.

[5] Taking the flow of air in these tunnels to be laminar is conservative in that it provides for minimal mixing and for maximum transport velocities. Any turbulent component would increase the former and reduce the latter effects.

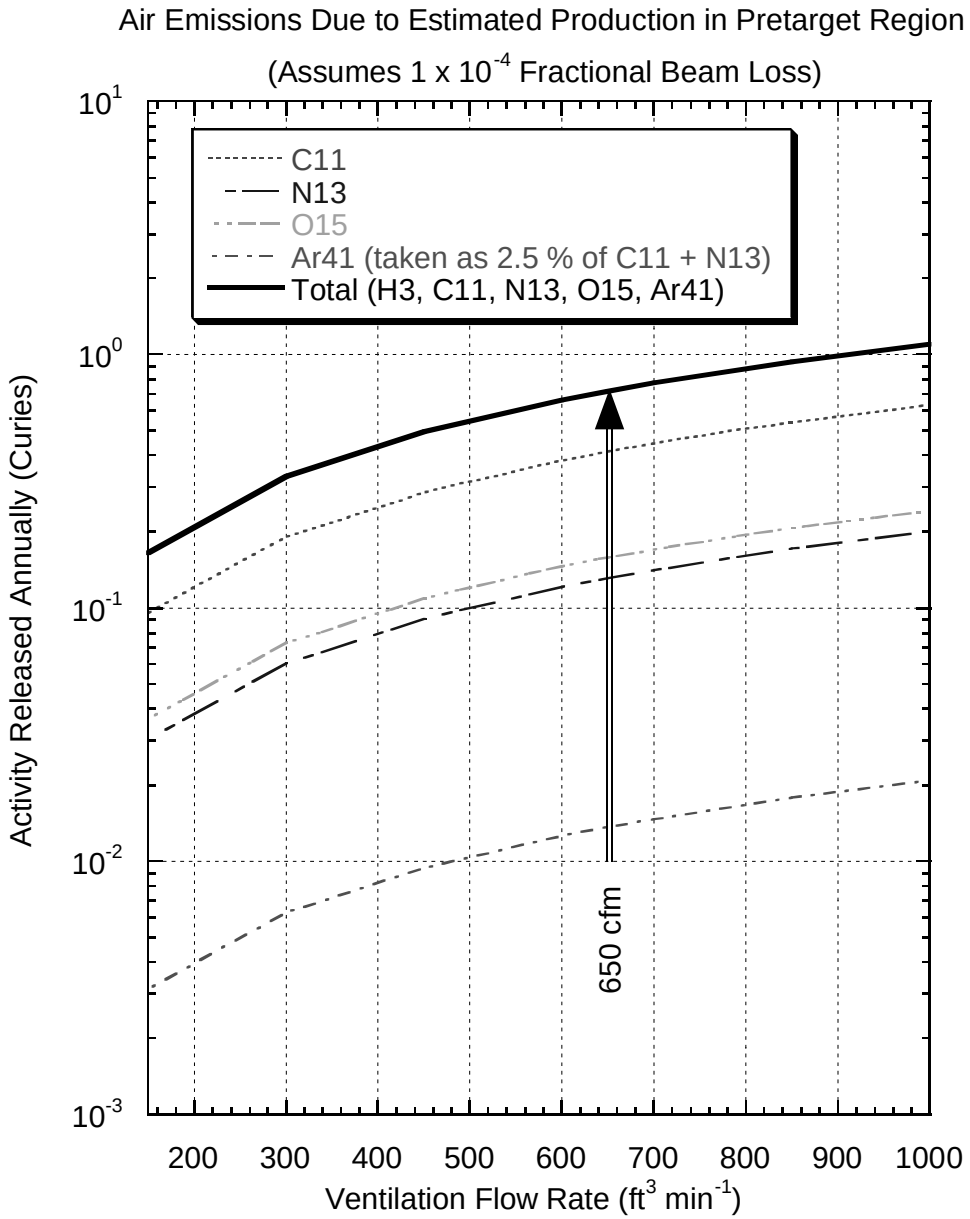

Figure 2 Calculated annual release of radioactivity produced in the Pretarget Region as a function of the ventilation flow rate in the Pretarget Region. The nominal value of the flow rate in the present design is 650 cfm and the corresponding results are indicated by the vertical arrow. For clarity, the annual release of ^{3}H is not shown on this graph. It increases linearly from 1.24×10^{-8} Ci yr^{-1} at 150 cfm to 8.25×10^{-8} Ci yr^{-1} at 1000 cfm. The results scale linearly with the fractional beam loss.

Target Hall

The region of the NuMI facility in which the largest amount of airborne radionuclides is produced is within the Target Hall. In this region of the facility large, open volumes are necessary to accommodate the primary proton target and the horn focussing system and their associated electrical and water connections. These open volumes are also located in the region where the largest flux densities of secondary particles are present along with the intense, uninteracted proton beam. Fortunately, it is possible to reduce these open volumes of air a great deal by using containers filled with helium gas at an approximate absolute pressure of one atmosphere.

James (Ja99) has performed calculations using the MARS code (Kr97) and modeling the Target Hall, Decay Region, and Hadron Absorber in detail. The model included those regions that are to be filled with helium. These simulations have provided the flux densities for the various volume regions within the target normalized per incident proton. Table 3 gives the volumes and normalized flux densities for these regions. For convenience, the various volume regions have been given numerical identifiers as well as a brief verbal description.

Table 3 Results of Target Hall Monte-Carlo Calculation for Different Volume Regions

Region No.	**Volume (cm^3)**	**Average Flux Density ϕ_{HE} (cm^{-2} proton^{-1})**	**Description of Region**
1	1.44×10^{2}	1.38	Inside baffle
2	5.29×10^{7}	3.94×10^{-8}	Air around baffle
3	4.23×10^{4}	1.60×10^{-2}	Air inside Horn One inner conductor
4	1.95×10^{7}	2.61×10^{-4}	Air inside Horn Two inner conductor
5	7.22×10^{7}	6.28×10^{-10}	Air above "TCapps"[6]
6	2.61×10^{8}	4.15×10^{-14}	Air in walkways
7	4.28×10^{8}	6.11×10^{-12}	Air in workspace
8	7.85×10^{7}	1.63×10^{-4}	In helium containers[7]

In order to maintain desirable conditions of humidity, it is planned to force circulation of the air in regions 1, 3, 4, and 5 collectively at the rate of 400 cfm. These regions are nominally sealed against leakage into the other 3 regions except for the pathway of the air used as part of the forced circulation system. These four regions correspond to the interior of the target station and include the critical components such as the focussing horns. It is clear from the flux densities that these four regions correspond to the areas of the most intense activation of air, as intuitively expected given their location. The circulated air would be supplied from the outer regions of the

[6] The "TCapps" region refers to the removable concrete shielding modules that are planned to be installed directly over the part of the target station containing the primary proton target and the horns.
[7] The production of ^{3}H in the helium containers (region 8) will be discussed separately later and in Appendix B.

target station. This internal air circulation system will serve to rapidly mix the air in these interior regions with the other air in the Target Hall. Any delaying effects resulting from this internal mixing have been ignored in the calculations presented here.

A Microsoft Excel™ spreadsheet was used to calculate the average concentrations within each of regions 1 through 7 by employing Eqs (1 - 3). The contributions of each of the seven regions to the total activity contained within the Target Hall were summed. The mixing of the air supplied to provide for the flow of air down through the decay region to the ventilation stack was taken into account by determining a value of *r* from the preliminary design parameters of the heating, ventilation, and air conditioning system. For a flow rate of 2250 cfm delivered at the downstream stack, a corresponding value of *r* of 2.7×10^{-4} s^{-1} (1 air change hr^{-1}) results. For other flow rates, including the presently selected value of 1500 cfm, the value of *r* was scaled accordingly (inverse to the flow rate). From these results, it was also straightforward to calculate the dose equivalent rate that might be received by a worker accessing the Target Hall. These results are provided in Appendix A.

The released activity was calculated by multiplying the resulting mixed concentrations of the radionuclides by the air flow rate to yield the rate of release of radioactivity from the Target Hall into the Decay Region. The transit time correlated with the inverse of the flow rate was taken into account in applying radioactive decay to the radionuclides prior to their release. During the transport through the Decay Region, the flow was assumed to be laminar. The nominal flow rate of 1500 cfm corresponds to an air exchange within the Target Hall enclosure of about 0.84 h^{-1}. Figure 3 shows the results of these calculations.

Separately, region 8 of Table 3 was used in order to estimate the buildup of radioactivity in the helium containers with time. ^{3}H is the only radionuclide that can be produced from helium target. According to Stevenson and Vincke (St98), a cross section of 30 mb is reasonable for the production of ^{3}H by high energy hadrons incident on helium. For this calculation, an irradiation time of one year (8760 hr) was chosen as representative of the time during which the helium containers would remain sealed. Applying Eq. (1), one obtains 0.18 Ci of ^{3}H in the containers at an average concentration of 2.29×10^{-9} Ci cm^{-3}. If the container were to suddenly burst, this activity would rapidly mix to a concentration in the Target Hall of 1.91×10^{-11} Ci cm^{-3}. This result does not include the further dilution by incoming air[8]. An estimate of the radiological hazard to a person present in this air can be obtained by comparison with the derived air concentration (DAC) for ^{3}H. Working in air containing radionuclides at one DAC corresponds to a effective dose equivalent rate of 2.5 mrem hr^{-1} (including internal deposition of ^{3}H). The DAC value for ^{3}H in the form of elemental hydrogen is 5×10^{-7} Ci cm^{-3} (CFR93). The concentration of ^{3}H that could be produced in the Target Hall is obviously completely trivial. A separate calculation of the ^{3}H production which verifies this particular result and also provides a check on the results of the Monte-Carlo calculations in general has been carried out by one of the authors (D. Boehnlein) (Bo98) and is provided in Appendix B.

[8] The concern of creating an oxygen deficiency hazard due to the presence of this volume of *gaseous* helium should be allayed by the fact that the helium volume comprises less than one per cent of the Target Hall air volume. Furthermore, given the fact that the helium containers would be filled at about one atmosphere absolute pressure, a leak of their contents could not occur instantaneously in any case.

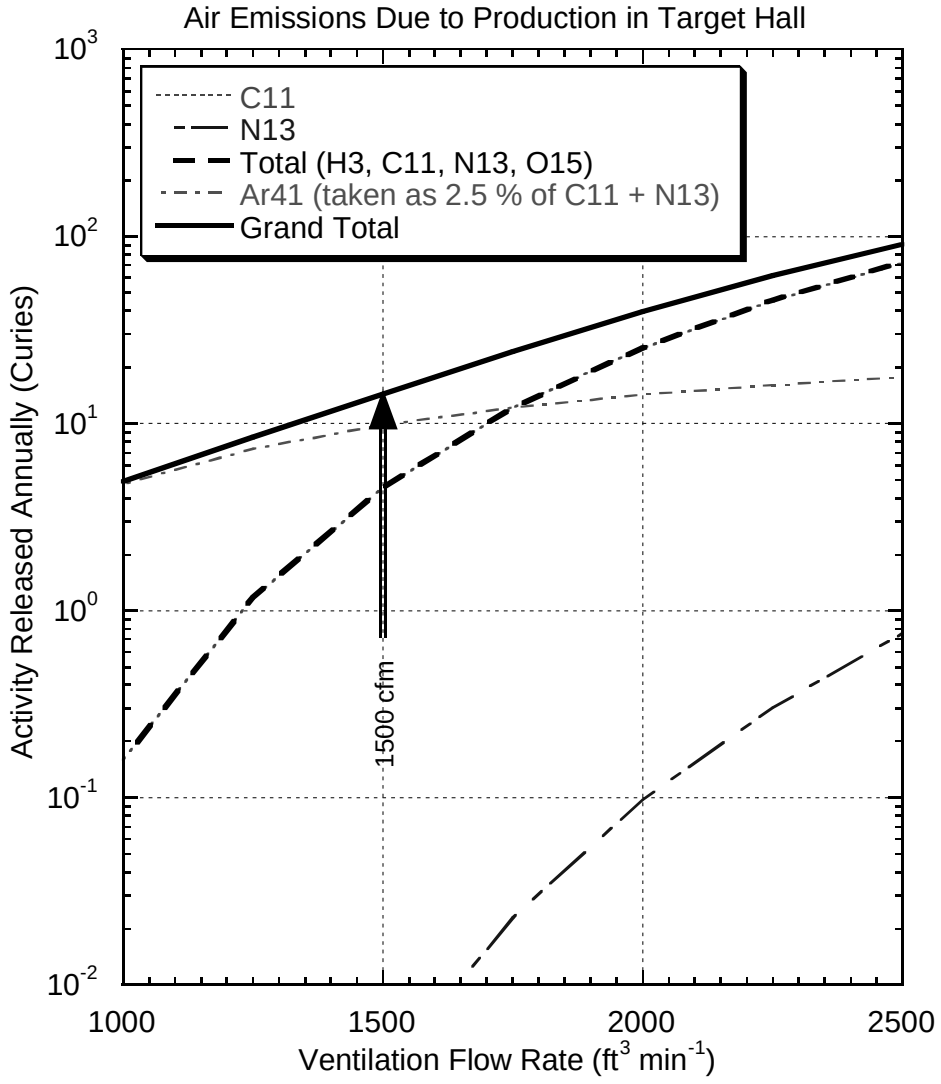

Figure 3 Calculated annual release of radioactivity produced in the Target Hall as a function of the ventilation flow rate in the upstream half of the Decay Region. The nominal value of the flow rate in the present design is 1500 cfm and the corresponding results are indicated by the vertical arrow. For clarity, the annual release of ^{3}H is not shown on this graph. This release has a value of about 2.57×10^{-7} Ci yr^{-1}, independent of the flow rate within the domain plotted. In this figure, the two curves labeled "C11" (thin short dashes) and "Total (H3, C11, N13, O15)" (thick longer dashes) are superimposed on each other over the domain plotted.

Decay Region

The Decay Region is similar to the Pretarget Region in that the air flow within it may be assumed to be laminar. This air flow in each half of the Decay Region is directly tied to that of adjacent Target Hall (upstream half) and the Hadron Absorber Region (downstream half). For this region, the results of the MARS calculation of James (Ja99) indicate the flux density, ϕ_{HE}, to be approximately uniform over the entire tunnel air volume of 3.12×10^{9} cm^{3} and has an average value of 2.05×10^{-13} cm^{-2} proton^{-1}. The same considerations pertain to the production and transport of these radionuclides as was discussed in connection with the Pretarget Region. Thus, Eq. (1) can be evaluated to determine the concentrations as a function of t_{irrad} and t_{cool}. The air flow rate is then multiplied by the concentration and by the time duration of the "operational year" to determine the annual release. Figure 4 displays the results of these calculations for each half of the Decay Region.

Hadron Absorber

The volume of air in this component is 1.42×10^{8} cm^{3}. The flux density of high energy hadrons, ϕ_{HE}, was found to be 1.21×10^{-9} cm^{-2} proton^{-1} in the calculation of James (Ja99). Using Eq. (1), the concentrations of the various radionuclides in the air within the Hadron Absorber were readily calculated. Assuming laminar flow, the release of these radionuclides from the ventilation stack was calculated by multiplying the concentrations by the product of the air flow rate and the time duration of the "operational year". The transit time correlated with the inverse of the flow rate was taken into account in applying radioactive decay to the radionuclides prior to their release. The results are provided in Figure 5.

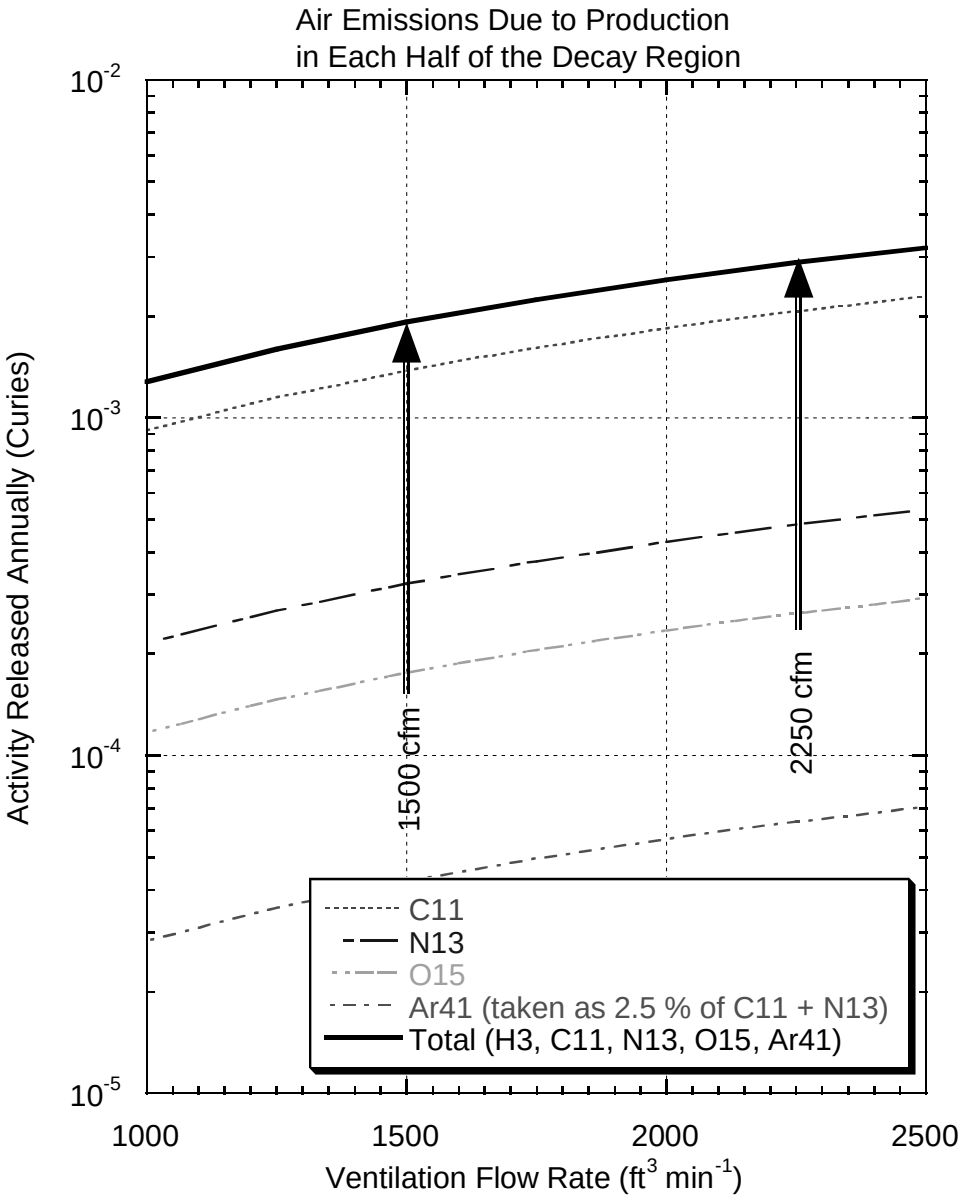

Figure 4 Calculated annual release of radioactivity produced in the Decay Region as a function of the ventilation flow rate for each half of this region. The nominal value of the flow rate in the present design for the upstream half of the Decay Region is 1500 cfm and for the downstream half is 2250 cfm. The corresponding releases of activity are indicated by the vertical arrows. For clarity, the annual release of ^{3}H from half of the Decay Region is not shown on this graph. It increases linearly from 3.29×10^{-8} Ci yr^{-1} at 1000 cfm to 8.23×10^{-8} Ci yr^{-1} at 2500 cfm.

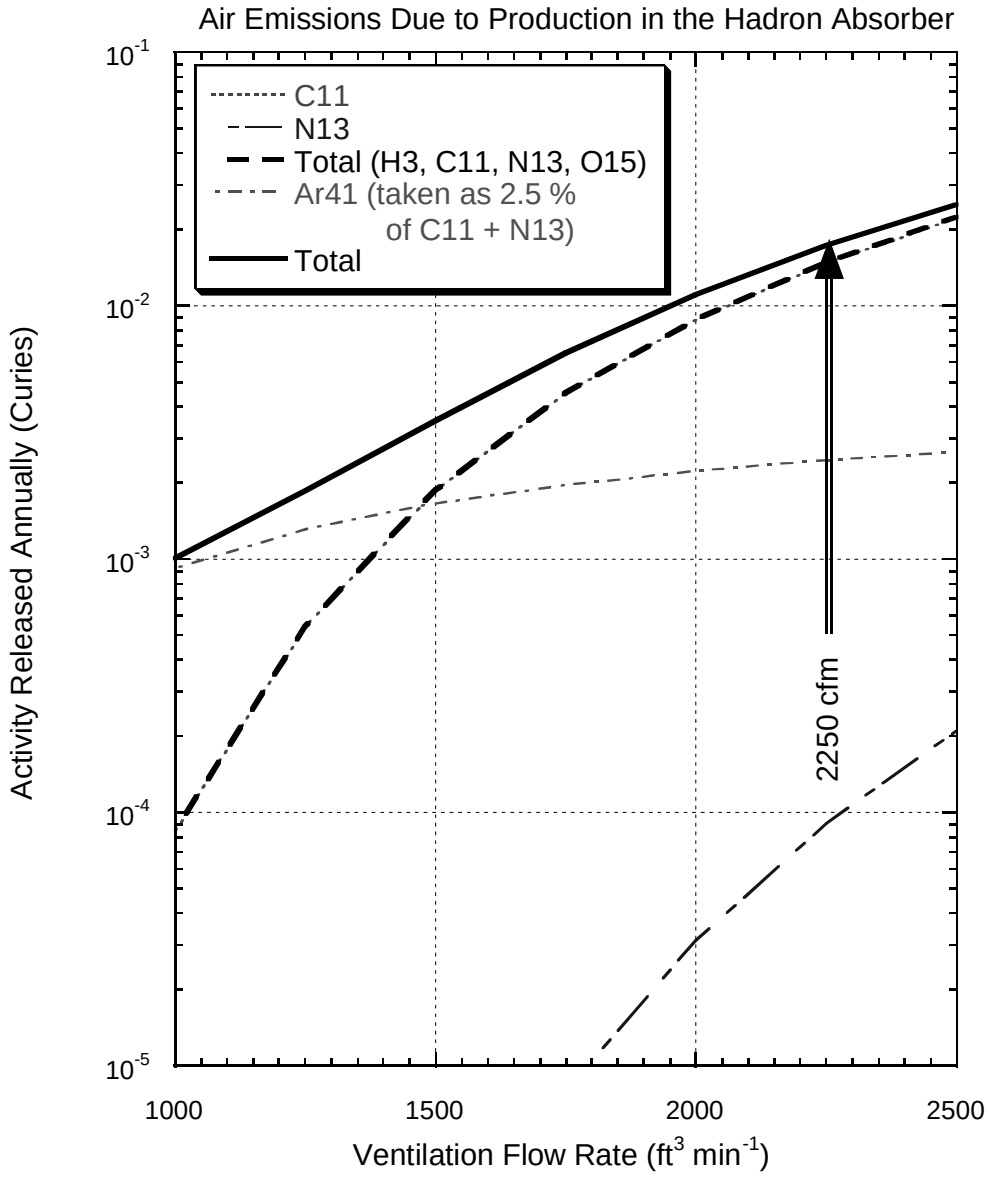

Figure 5 Calculated annual release of radioactivity produced in the Hadron Absorber as a function of the ventilation flow rate in the downstream half of the Decay Region. The nominal value of the flow rate in the present design for the downstream half of the Decay Region is 2250 cfm and the corresponding results are indicated by the vertical arrow. For clarity, the annual release of ^{3}H is not shown on this graph. This release has a value of about 2.26×10^{-8} Ci yr^{-1}, independent of the flow rate within the domain plotted. In this figure, the two curves labeled "C11" (thin short dashes) and "Total (H3, C11, N13, O15)" (thick longer dashes) are superimposed on each other over the domain plotted.

Conclusion

The results of these estimates of the annual releases of the various radionuclides are given in Table 4, which presents the contributions of these various sources at the nominal ventilation rates shown. The releases of activity produced in each half of the Decay Region are tabulated separately, due to the differences in ventilation rates for the two halves.

Table 4 Summary of Annual Releases of Radionuclides (Curies) for the Various Regions of the NuMI Facility.

Region	**Assumed Flow Rate (cfm)**	**^{3}H**	**^{11}C**	**^{13}N**	**^{15}O**	**^{41}Ar**	**Total**
Pretarget	650	5.36×10^{-8}	4.14×10^{-1}	1.31×10^{-1}	1.58×10^{-1}	1.36×10^{-2}	7.18×10^{-1}
Target Hall	1500	2.75×10^{-7}	4.57	3.37×10^{-3}	0	9.82	14.39
Decay Region-1st half	1500	4.94×10^{-8}	1.38×10^{-3}	3.23×10^{-4}	1.76×10^{-4}	4.26×10^{-5}	1.92×10^{-3}
Decay Region-2nd half	2250	7.41×10^{-8}	2.07×10^{-3}	4.84×10^{-4}	2.64×10^{-4}	6.38×10^{-5}	2.88×10^{-3}
Absorber	2250	2.26×10^{-8}	1.48×10^{-2}	9.06×10^{-5}	0	2.46×10^{-3}	1.73×10^{-3}
Totals		**5.24×10^{-7}**	**5.00**	**1.36×10^{-1}**	**1.59×10^{-1}**	**9.84**	**15.13**
Per Cent		3.5×10^{-6}	33.03	0.90	1.049	65.02	

The dominance of ^{41}Ar is principally due to the long transit time for the air moving from the Target Hall to the Decay Region ventilation stack. It is concluded that the goal of keeping the annual emissions of airborne radionuclides from the NuMI facility below 45 Ci can readily be met. The need to minimize the thermalization of neutrons to the extent practicable in order to control the production of ^{41}Ar is clearly evident. These results indicate that the maximum annual dose equivalent at the Fermilab site boundary due to the operations of NuMI will be approximately 0.0085 mrem. The ventilation should be provided according to present design plans. In this paper, we have not considered airborne radioactivity produced and released due to beam losses in the extraction region of the Fermilab Main Injector. Initial calculations of these effects have been reported by Drozhdin, et al. (Dr99) and further development of these calculations are planned. In view of the results of this paper, these studies should continue and should specifically include predictions of the release of airborne radionuclides. They may also be helpful in further refining the estimates for the Pretarget Region of the NuMI facility.

Acknowledgments

We would like to thank C. James for providing the Monte-Carlo results used as the basis for the majority of these calculations. We would also like to thank L. Hammond for his insight on the ventilation system and A. Elwyn, D. Grobe, and K. Vaziri for their critical comments on this paper.

Appendix A
Calculation of Effective Dose Equivalent Rate Due to Activated Air in the Target Hall

The concentrations found with the target station volume, after uniformly mixing the contributions of the regions of Table 3, were used to calculate the effective dose equivalent rate due to exposure to this air. This was done by taking the concentrations for each radionuclide of concern, including ^{7}Be, calculated at the end of the irradiation, $C_i(0)$, dividing them by the appropriate Derived Air Concentrations (DACs) for occupational workers, and summing them to determine the total fraction of a DAC achieved (see discussion of DACs in the main text). The effective dose equivalent rate, $dH(t_{cool})/dt$, as a function of decay time, t_{cool}, is thus given by,

$$\frac{dH(t_{cool})}{dt} = 2.5\sum_i \frac{C_i(0)}{DAC_i}\exp[-(\lambda_i + r)t_{cool}], \qquad \text{(mrem hr}^{-1}\text{)}, \qquad (8)$$

since the exchange of air reduces the concentration of air in a manner similar to that provided by the radioactive decay. The results are plotted in Fig. 6 as a function of time after beam shutdown for the nominal flow rate of 1500 cfm. It is seen that this dose equivalent rate rapidly decays to trivial levels after only about an hour of cooldown.

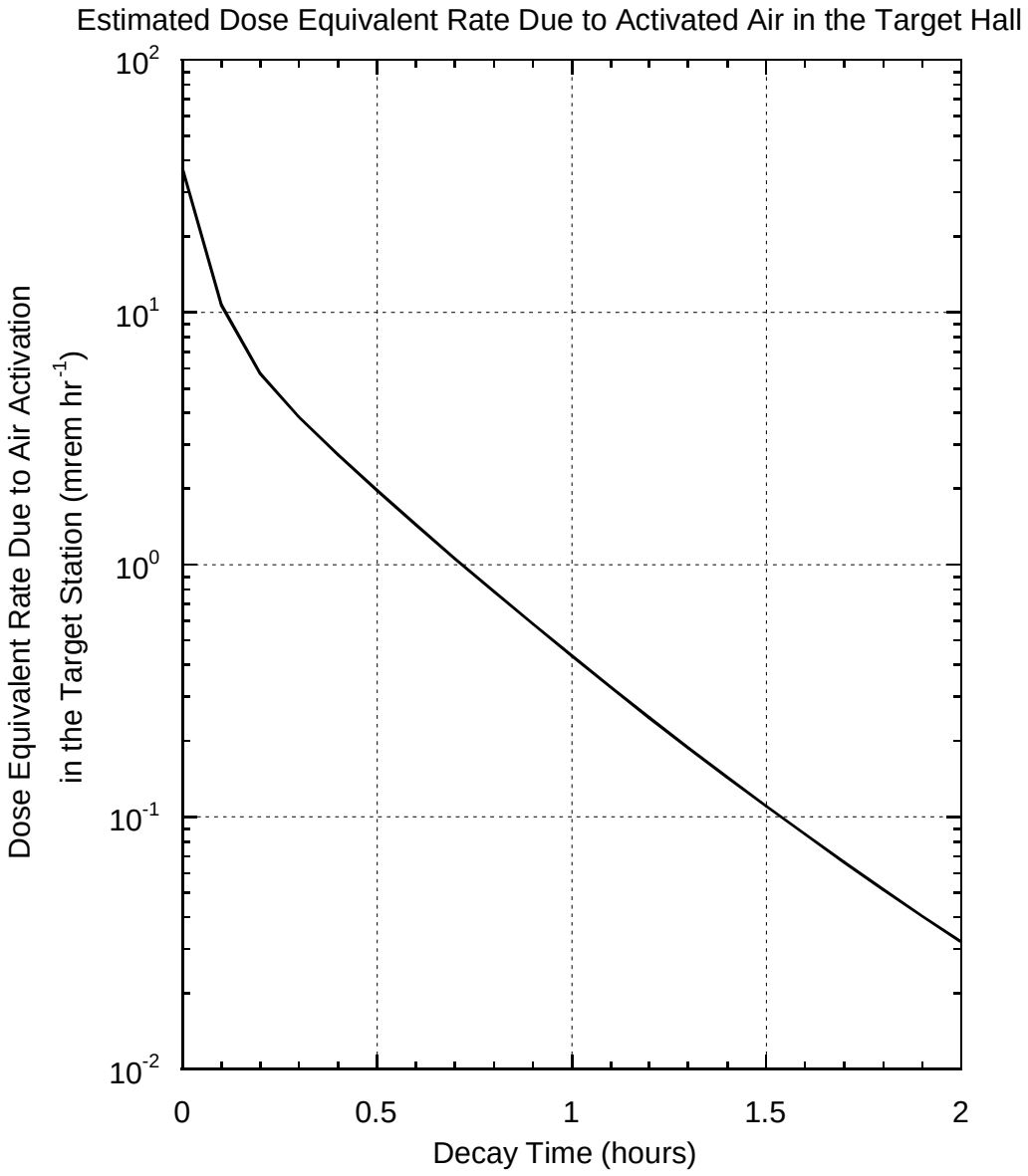

Figure 6 Estimated dose equivalent rate due to activated air in the Target Hall as a function of time after beam turnoff at the nominal value of the flow rate of 1500 cfm.

Appendix B
Calculation of the Production of ^{3}H in the Helium Containers

This section updates a calculation by one of the authors (D. Boehnlein) and previously documented as a NuMI Note (Bo98). The long flight path of a high intensity hadron beam through air creates the potential for levels of air activation higher than any previously produced at Fermilab. It is proposed to partially mitigate the air activation in the target hall by installing a series of helium-filled containers along the flight path of the secondary beam. During the preparation of the Preliminary Safety Assessment Document (PSAD) for NuMI, the question was raised as to whether the NuMI beam would generate a significant amount of tritium within the containers through interactions with the helium. An estimate is calculated below which, of course, starts with the high energy term in Eq (1) which is limited to the production of the one possible radionuclide, ^{3}H. Several simplifying assumptions will now be made:

A) The production of tritium is dominated by hadronic spallation reactions, without significant contributions from reactions involving leptons, photons or secondary processes. This assumption is reported by Sullivan (Su92) to hold true for radionuclide production in air and eliminates the first two summations in Eq. (1).

B) The cross section for tritium production is essentially the same for all hadrons. This is reasonable given that spallation is a strong interaction. This approximation eliminates the need to perform a summation over particle types to calculate Φ.

C) The spallation cross section is essentially independent of the hadron energy above 100 MeV (Su92).

Determination of N is straightforward from Avogadro's number, N_A, the density, ρ, and atomic weight, M, of helium:

$$N = \frac{\rho}{M} N_A = \frac{1.79 \times 10^{-4} \text{ g cm}^{-3}}{4.00 \text{ g mol}^{-1}} \times 6.02 \times 10^{23} \text{ mol}^{-1} = 2.69 \times 10^{19} \text{ cm}^{-3}. \qquad (9)$$

Deciding on a value for σ is less straightforward and represents the major uncertainty in this estimation. As of this writing, no measured cross section for the production of tritium through hadronic spallation of helium is available. However, tritium production cross sections have been compiled for reactions with other targets by Konobeyev and Korovin (Yo93). Plots of σ vs. atomic number A show the cross section falling sharply for light elements. Variation of the cited values for A between 10 and 15 make the exact slope of the falloff difficult to determine, although a visual inspection might place the cross section for $A = 4$ as low as 5 mb or as high as 30 mb. Twenty mb is chosen here as a reasonable, yet conservative, guess. As stated in the main text, Stevenson and Vincke (St98) have used a value of 30 mb.

The following assumptions are made in estimating Φ based upon the beam intensities discussed above for a run of two years as planned by the MINOS experiment (MI95). The protons are incident on a target of approximately two interaction lengths (Hy97), hence 86.5% of the protons will produce secondary particles. The number of secondaries is estimated from a plot presented by Sullivan (Su92), which shows this number vs. angle of emission for a range of beam energies. From the conceptual design of the NuMI Target Hall, the half-angle of the cone subtended by the helium bags is estimated to be 3.5°. Visual inspection of Sullivan's plot for this angle and a beam energy of 120 GeV results in an estimate of 5 secondary hadrons traversing the helium bags per interacting proton. The average flux density is obtained by dividing the sum of the secondary hadrons and non-interacting protons by the cross-sectional area of the helium bags, assumed here to be 10^4 cm^2.

$$\Phi = \frac{7.4\times 10^{20}\left[(5\times .865)+.135\right]}{10^4\ \text{cm}^2} = 3.30\times 10^{17}\ \text{cm}^{-2}. \qquad (10)$$

The fluence will be effectively increased because of tertiary hadrons produced by interactions in the helium itself. The number of tertiaries, according to Sullivan (Su92) is given by

$$Q = 16E^{0.15} - 10, \qquad (11)$$

where E is the hadron energy in GeV. Two simplifying assumptions, which increase the conservatism of the estimate, are made regarding the tertiary hadrons. Firstly, all hadrons producing tertiaries are assumed to have E = 120 GeV. Secondly, the number of target atoms N is assumed to be the same for tertiaries as it is for the other hadrons, although it is actually less for all tertiaries except those produced in the forward direction at the upstream end of the helium bags. The first assumption results in an estimate of 22.8 tertiaries per interaction. Since the helium in the containers comprises about 1.4% of an interaction length, the effective flux density, Φ_e, is,

$$\Phi_e = 3.30\times 10^{17}\ \text{cm}^{-2}\left[1+(.014)(22.8)\right] = 4.35\times 10^{17}\ \text{cm}^{-2}. \qquad (12)$$

Combining these equations along with the estimated cross section gives the concentration of tritium atoms:

$$\begin{aligned} S &= \left(2.69\times 10^{19}\ \text{cm}^{-3}\right)\left(2\times 10^{-26}\ \text{cm}^{2}\right)\left(4.35\times 10^{17}\ \text{cm}^{-2}\right)\left[1-e^{-(.0564/\text{yr})(2\ \text{yr})}\right]. \\ &= 2.50\times 10^{10}\ \text{cm}^{-3} \end{aligned} \qquad (13)$$

Converting the decay constant of tritium into sec^{-1}, the specific activity of tritium in the helium bags is given by

$$A = S\lambda = \left(2.50\times 10^{10}\ \text{cm}^{-3}\right)\left(1.79\times 10^{-9}\ \text{s}^{-1}\right) = 44.8\ \text{Bq ml}^{-1} = 1.21 \text{ x } 10^{-3}\ \mu\text{Ci cm}^{-3}. \qquad (14)$$

The chemical form of the tritium would depend on the type and amount of contaminants (oxygen, nitrogen, etc.) in the helium. As stated earlier, the dominant uncertainty in this estimate is in the selection of σ. Other reasonable values used in the calculation above could give a value of A between 11 Bq/ml (0.3×10^{-3} μCi cm^{-3}) and 70 Bq/ml (1.9×10^{-3} μCi cm^{-3}). These compare very well with the value of 2.29×10^{-3} μCi cm^{-3} derived from the results of the MARS calculation, where σ = 30 mb was assumed. However, as shown below, these differences would not make a difference in the conclusion of this calculation.

From the standpoint of environmental protection, one should consider the total amount of tritium that would build up into the container and that could potentially be released. The total amount of radioactivity vented from the helium bags would be

$$R = \left(5 \times 10^{7}\ \text{cm}^{3}\right)\left(44.8\ \text{Bq cm}^{-3}\right)\left(2.70 \times 10^{-11}\ \text{Ci Bq}^{-1}\right) = 0.06\ \text{Ci}. \qquad (15)$$

This calculation was performed for σ = 20 mb. If one adjusts the results to σ = 30 mb and scales by the volume of 7.85×10^{7} cm^3 used in conjunction with the MARS calculation, the result is a total activity of 0.14 Ci. Thus, this semiempirical approach is in excellent agreement with that obtained using MARS.

References

(Aa86) P. Aarnio, A. Fassò, H. J. Moehring, J, Ranft, and G. R. Stevenson, "FLUKA 86 user's guide", CERN Divisional Report TIS-RP/190, 1986 and P. A. Aarnio, J. Lindgren, J. Ranft, A. Fassò, G. R. Stevenson, "Enhancements to the FLUKA 86 program (FLUKA 87), CERN Divisional Report, TIS-RP/190, 1987. This reference is for the version of the code used in the calculations reported by Schopper et al. (Sc90).

(Ba69) M. Barbier, *Induced radioactivity*, (North-Holand Publishing Company, Amsterdam and London, Wiley Interscience Division, John Wiley and Sons, Inc, New York, 1969).

(Bo98) D. J. Boehnlein, "An estimation of tritium production in helium bags in the NuMI Target Hall", NuMI Note 371, April 1998.

(Bu89) S. W. Butala, S. I. Baker, and P. M. Yurista, "Measurements of radioactive gaseous releases to air from target halls at a high-energy proton accelerator", Health Physics 57 (1989) 909-916.

(CFR89) United States Code of Federal Regulations, Title 40, Part 61, Subpart H, "National emissions standard for hazardous air pollutants (NESHAP) for the emission of radionuclides other than radon from Department of Energy Facilities", 1989.

(CFR93) United States Code of Federal Regulations, Title 10, Part 835, "Occupational Radiation Protection [at DOE Facilities]", 1993. Note: Regulatory agencies commonly round off unit conversions in tables of standards.

(Co99) J. D. Cossairt, "Radiation physics for personnel and environmental protection", Fermilab Report TM 1834, February 1999.

(Da84) R. J. Dagenais, "A study of the accumulation and reduction of radon and its daughter products in an underground tunnel", Fermilab Radiation Physics Note, 46, August 1984.

(Dr99) A. I. Drozhdin, P. W. Lucas, N. V. Mokhov, C. D. Moore, and S. I .Striganov, "Radiation environment resulting from Main Injector beam extraction to the NuMI beam line", presented at the 1999 Particle Accelerator Conference, New York, New York, March 29-April2, 1999, FERMILAB-Conf-99/061.

(El86) A. J. Elwyn and J. D. Cossairt, "A study of neutron leakage through an Fe shield at an accelerator", Health Phys. 51 (1986) 723-735.

(Hy97) J. Hylen, et al., "Conceptual design for the technical components of the Neutrino Beam for the Main Injector (NuMI)", Fermilab TM-2018 (1997).

(Ja99) C. James, private communication, March 17, 1999.

(Ko93) A. Yu. Konobeyev and Yu. A. Korovin, "Tritium production in materials from C to Bi irradiated with nucleons of intermediate and high energies", Nucl Instr. and Meth. in Phys. Res. B82 (1993) 103-115.

(Kr97) O. Krivosheev and N. V. Mokhov, "A new MARS and its applications", Fermilab-Conf-98/043 (1998).

(Lu99) P. W. Lucas, private communication (May 1999).

(MI95) The MINOS Collaboration, "A long-baseline neutrino oscillation experiment at Fermilab", Fermilab Proposal P-875 (1995),

(Mo99) N. Mokhov, private communications (May 1999).

(NuMI98) *The NuMI facility technical design report*, Revision 1, Fermilab, October 1998.

(Pa73) H. W. Patterson and R. H. Thomas, *Accelerator health physics,* Academic Press, New York, 1973.

(Sc90) H. Schopper (editor), A. Fassò, K. Goebel, M. Höfert, J, Ranft, and G. Stevenson, *Landolt-Börnstein numerical data and functional relationships in science and technology new series; Group I: Nuclear and particle physics Volume II: Shielding against high energy radiation* (O. Madelung, Editor in Chief, Springer-Verlag, Berlin, Heidelberg, 1990).

(St98) G. R. Stevenson and H. H. Vincke, "Initial estimates of radiological parameters of environmental interest for the CERN/INFN Gran-Sasso neutrino project", European Organization for Nuclear Research Report CERN/TIS-RP/IR/98-13 (May 1998).

(Su92) A. H. Sullivan, *A guide to radiation and radioactivity levels near high energy particle accelerators* (Nuclear Technology Publishing, Kent, England, 1992).

(Th88) R. H. Thomas and G. R. Stevenson, "Radiological safety aspects of the operation of proton accelerators", Technical Report No. 283, International Atomic Energy Agency, Vienna, 1988.

(Va93) K. Vaziri, V. Cupps, D. Boehnlein, D. Cossairt, A. Elwyn, and T. Leveling, "AP0 stack monitor calibration", Fermilab Radiation Physics Note #106, May 1993.

(Va94) K. Vaziri, V. R. Cupps, D. Boehnlein, D. Cossairt, and A. Elwyn, "A detailed calibration of a stack monitor used in the measurement of airborne radionuclides at a high energy proton accelerator", Fermilab Report FERMILAB-Pub-96/037, 1996.